DTU Library

Tools for Multimode Quantum Information: Modulation, Detection, and Spatial Quantum Correlations

Lassen, Mikael Østergaard; Delaubert, Vincent; Janousek, Jirí; Wagner, Kate; Bachor, Hans. A-; Lam, Ping Koy; Treps, Nikola; Buchhave, Preben; Fabre, Claude; Harb, Charles

Link back to DTU Orbit

Tools for Multimode Quantum Information:
Modulation, Detection, and Spatial Quantum Correlations

M. Lassen,[1,2] V. Delaubert,[1,3] J. Janousek,[1,2] K. Wagner,[1] H.-A. Bachor,[1] P. K. Lam,[1] N. Treps,[2]
P. Buchhave,[2] C. Fabre,[3] and C. C. Harb[4,1,*]

[1]*Australian Center for Quantum-Atom Optics, The Australian National University, Canberra ACT 0200, Australia*
[2]*Department of Physics, DTU, Building 309, 2800 Lyngby, Denmark*
[3]*Laboratoire Kastler Brossel, 4 place Jussieu, case 74, Paris 75252 Cedex 05, France*
[4]*School of Information Technology and Electrical Engineering, University College, The University of New South Wales,
Canberra, ACT, 2600*

We present the key elements required for continuous variable parallel quantum information protocols based on spatial multimode quantum correlations. We describe techniques for encoding, combining and detecting spatial quantum information with high efficiency in the individual transverse modes. Until now, the missing feature for the implementation of such protocols was the generation of squeezing in higher order transverse Hermite-Gauss modes. We experimentally demonstrate squeezing in selective modes by fine-tuning the phase matching condition of the nonlinear $\chi^{(2)}$ material and the cavity resonance condition of an optical parametric amplifier. Combined, these results open the way to practical multimode optical quantum information systems.

PACS numbers: 42.50.Dv, 03.67.−a

Optical quantum communication and information processing is developing rapidly [1]. Both single photon and continuous variables (CV) are being used, already enabling the generation, transmission, and detection of quantum correlations. CV optical techniques include close to perfect modulation and detection schemes, which is a requirement for the effective use of squeezed and entangled light [2–5] for applications such as sensing and gravitational-wave detection [6,7], quantum communication and teleportation [8], dense coding [9], secret sharing [10], noiseless amplification [11], and possibly quantum logic [12].

So far, CV techniques typically use a single mode and a pair of conjugate quantum parameters per beam: mean field amplitude and phase quadratures or polarization parameters. Using this set of variables, several key elements are required to implement quantum information protocols. The first one is the efficient signal encoding of the individual conjugate observables, and is typically achieved with electro-optic modulation (EOM) of the sidebands at frequency Ω around the central laser frequency ν_L. These sidebands can be used to carry the information. Second, CV schemes use high efficiency phase sensitive detectors, such as homodyne detectors, that allow the interrogation of each quadrature individually. Finally, they require squeezed light, i.e., pairs of quantum correlated sidebands at frequency $\nu_L \pm \Omega$, allowing performances with signal to noise ratio better than the conventional quantum noise limit (QNL), and the generation of quadrature or polarization entanglement [13].

CV experiments have traditionally been performed with TEM_{00} profile for the squeezed beam and the homodyne detection local oscillator (LO). At the same time, parallel research efforts into CV quantum imaging have been de-

veloped [14], and concentrated on the transmission, amplification, and processing of spatial information with quantum correlations [15,16]. Recent results include the detection of spatial parameters such as small displacements below the QNL [17], the optimization of imaging techniques [18], and proposals for more advanced applications such as super-resolution [19] and quantum holography [20].

The aim of our research is to use the spatial properties of light to demonstrate that one optical beam can convey several independent channels of quantum information. This can be used for quantum communication or spatial sensing, as suggested in Figs. 1(a) and 1(b), respectively. Such multimode systems have advantages in regard to the complexity of the protocols [21]. This work with continuous variables complements the single photon systems, designed to transmit not just qubits but qudits, which use photon states with different angular momenta [22,23].

Here we present all the key elements required for extending CV quantum optics from the single mode case to a multimode system. The quantum channels are provided by the TEM_{nm} Hermite-Gauss (H-G) modes. The orthogonality of these modes allows us to address the parallel channels individually and to combine them with minimal loss and negligible crosstalk. Second, we report more than 90% detection efficiencies of the individual channels. Finally, we describe how to efficiently generate spatially squeezed light in higher order H-G modes. Together these achievements provide a complete multimode quantum information system and demonstrate its efficiency.

For our investigation, we focus on the lowest order H-G modes: TEM_{00}, TEM_{10}, and TEM_{20}. These modes are directly related to small spatial variations of a Gaussian
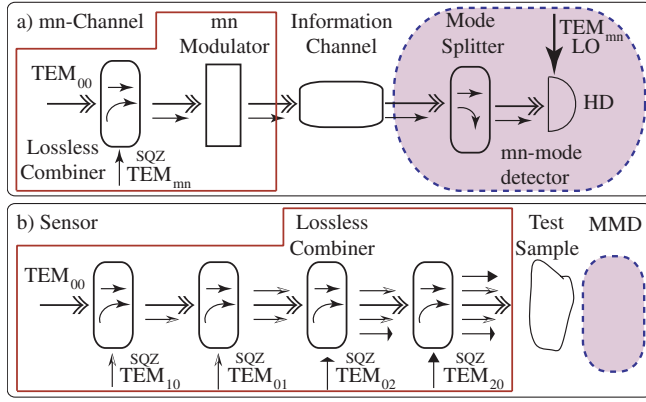
FIG. 1 (color online). Practical spatial multimode systems:
(a) single quantum information channel including modulation,
propagation, and detection scheme in the case of information
encoded on a TEM$_{mn}$ mode; (b) measurement of the spatial
properties of a test sample using lossless combiners and multi-
mode detectors (MMD). SQZ: squeezed. HD: homodyne detec-
tion.

beam [24]. In particular, the real and imaginary parts of the
TEM$_{10}$ mode represent changes in transverse position δd
and tilt $\delta \theta$ of a TEM$_{00}$ beam [25], whereas the real and
imaginary parts of the TEM$_{20}$ mode are related to a waist
size mismatch δw and a waist position mismatch along the
propagation axis δz. The following equation quantifies
these relationships:

$$E(x) = A_0 \left[u_0(x) + \left(\frac{\delta d}{w_0} + i \frac{\pi w_0 \delta \theta}{\lambda} \right) u_1(x) + \frac{\delta w}{\sqrt{2} w_0} u_2(x) \right.$$
$$\left. + i \frac{\delta z \lambda}{2\sqrt{2} \pi w_0^2} \left(\frac{5}{\sqrt{2}} u_0(x) + u_2(x) \right) \right],$$

where the spatial function $u_n(x)$ refers to the profile of the
TEM$_{n0}$ mode. A_0 is the average amplitude, w_0 is the waist
size, and λ is the wavelength. Similar beam properties
along the orthogonal transverse coordinate y are carried
by the TEM$_{01}$ and TEM$_{02}$ modes. We can encode infor-
mation directly into the transverse orthogonal modes with
close to perfect efficiency using simple electro-optic or
mechanical spatial modulators acting on a TEM$_{00}$ beam,
such as a piezoelectric device, a tilted EOM, or a movable
lens [17,26].

For combining and analyzing orthogonal modes without
loss, as schematically shown in Fig. 1(a), we can use a high
finesse ring cavity, or alternatively a planar Mach Zehnder
interferometer, parallel to x or y, with an odd number of
mirrors, in order to combine even and odd modes. We have
demonstrated in our earlier work more than 95% efficiency
for these components [17,26]. We thus have the ability to
synthesize a multimode laser beam which combines the
TEM$_{00}$ mode with the higher order transverse modes
TEM$_{01}$, TEM$_{10}$, TEM$_{02}$, and TEM$_{20}$. The resulting combi-
nation provides each channel with two quadratures of a

conjugate pair of quantum variables, as shown in Fig. 1(a)
in the case of a single channel carried by the TEM$_{nm}$ mode.
It is then straightforward to extend this scheme to several
quantum channels. A similar scheme presented on Fig. 1(b)
can be used as a sensor for spatial modification. Here a
multimode squeezed beam is incident on a sample and
detected with a multimode detector (MMD), which corre-
sponds to cascaded single channel detectors presented in
Fig. 1(a). Each channel provides information on a specific
spatial property of the sample with sub-QNL precision.

The detection of these modes requires special attention.
Conventional spatial detectors, such as split detectors or
diode arrays, are simple but provide only limited effi-
ciency. For example, the best theoretical efficiency of a
split detector for displacement measurements is only 64%
in intensity [25]. In contrast, with "spatial" homodyne
detectors which use a LO beam that is mode matched to
the specific TEM$_{nm}$ channel, we reported more than 96%
detection efficiency [26].

The crucial component missing until recently was the
efficient generation of squeezing in the TEM$_{nm}$ modes. We
propose here to fill this technology gap by showing that the
phase matching of a type I second order nonlinear process
can be used to selectively choose the spatial profile of the
squeezed mode, using an optical parametric amplifier
(OPA). An OPA is a phase dependent device which,
when operated below threshold, can reduce the noise in
one quadrature to below the QNL (squeezing), while the
conjugate quadrature shows extra noise (antisqueezing).
This was first demonstrated by Wu *et al.* in 1986 [27].
Since then OPAs have reliably produced up to -7 dB of
squeezing [28,29].

Producing squeezed light in any of the TEM$_{nm}$ modes
using an OPA requires the optimization of three conditions.
First, the OPA resonator needs to be resonant for the H-G
mode of interest. This is simply achieved by misaligning a
TEM$_{00}$ seed beam in order to couple light into the desired
component and to lock the length of the cavity to its
resonance. Second, the spatial profiles of the pump beam,
at frequency $2\nu_L$, and the seed beam, at frequency ν_L, need
to be chosen to maximize the spatial overlap and at the
same time the nonlinear gain of the down-conversion
process. Finally, phase matching has to be set to favor
the conversion into the required spatial mode.

To understand how to optimize the last two conditions,
let us now concentrate on the reverse process of optical
parametric amplification, namely, second harmonic gen-
eration (SHG). When such systems are operated with
higher order spatial modes, optimal phase matching occurs
at different crystal temperatures, since each mode acquires
different Gouy phase shift, when propagating through the
nonlinear medium. As a demonstration of this effect, we
pump a single pass SHG with a TEM$_{n0}$ pump mode, as
shown in the upper part of Fig. 2. We use a MgO:LiNbO$_3$
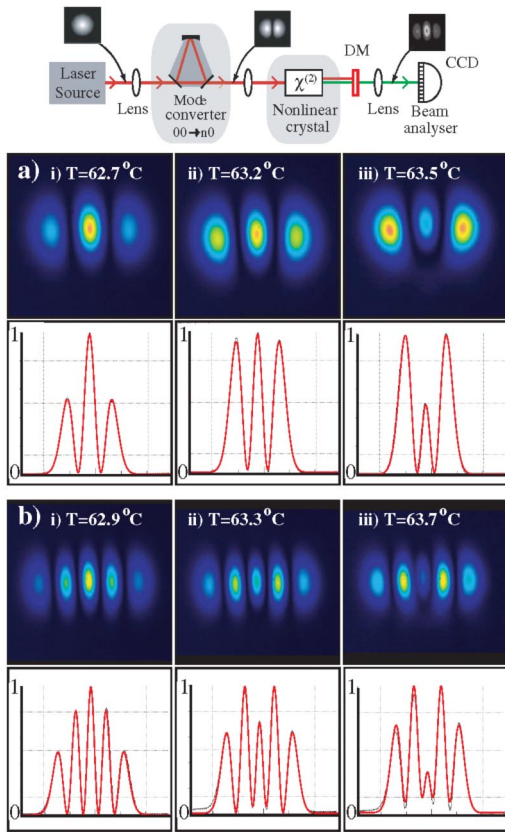lithium niobate crystal, whose birefringence is highly tem-

FIG. 2 (color).   Top: Scheme for single pass SHG measurement in the case of TEM$_{10}$ fundamental mode operation. Below: SH profiles generated in the crystal far field for three phase matching temperatures with a (a) TEM$_{10}$ and (b) TEM$_{20}$ pump profile. The cross-section traces show excellent between experimental results and theory fits.

perature dependent, and therefore allows adjustment of the phase matching condition for a particular spatial mode. The TEM$_{n0}$ pump mode, produced at 1064 nm by a diode-pumped NPRO Nd:YAG laser, is generated by misaligning a ring cavity, designed to prevent any transverse mode degeneracy and locked to the resonance of the TEM$_{n0}$ mode. This mode converting device delivers a pure transverse TEM$_{n0}$ output mode, which is focused into the crystal such that $z_R = l/2$, where z_R is the beam Rayleigh range and l is the crystal length. A dichroic mirror, DM, is used to filter out the fundamental pump field, and the second harmonic (SH) profile is detected with a CCD camera in the far field.

The generated SH spatial profiles, normalized to their maximum, are presented for different crystal temperatures in Figs. 2(a) and 2(b) for TEM$_{10}$ and TEM$_{20}$ pump modes, respectively. The spatial distribution of the SH field varies strongly with the crystal temperature. Tuning the temperature allows reproducible control over the conversion into other TEM$_{n0}$ modes. In the case of a TEM$_{10}$ pump the SH field can be tuned from a predominantly TEM$_{00}$ to a predominantly TEM$_{20}$ profile, as shown in Fig. 2(a).

Similarly, for the TEM$_{20}$ pump mode the SH field is a temperature dependent linear combination of the TEM$_{00}$, TEM$_{20}$, and TEM$_{40}$ modes, as shown in Fig. 2(b). For a comparison of the experimental data with a quantitative model, we calculate the mode overlap between the TEM$_{n0}$ modes [30]. We predict the spatial intensity distribution of the SH light for the different temperatures, as shown in Fig. 2 in the lower diagrams together with the experimental profiles. They are in excellent agreement and show the tunability of the mode composition via crystal temperature.

We use this technique for the generation of squeezed light. As SHG and OPA operation are reverse processes, the SH beam profiles presented in Fig. 2 correspond to the optimal pump shape for OPA operation for a given crystal temperature. Optimal conversion efficiency is expected when the pump profile corresponds to the square of the fundamental. Although generating such a complicated beam to pump the OPA is possible by using holograms [31] or a spatial light modulator, at the cost of reduced parametric interaction, we choose to simply use the TEM$_{00}$ mode delivered by our dual input laser at 532 nm, and optimize the crystal temperature for this operation. A schematic diagram of our experimental setup to generate squeezing in higher order modes is presented in Fig. 3. All the technical details are presented in Ref. [30].

The measured squeezing in the three lowest order H-G modes is shown in Fig. 4 with a resolution bandwidth of 300 kHz and a video bandwidth of 300 Hz. All traces are normalized to the QNL, given by trace (ii), which is measured by blocking the squeezed beam before the homodyne detector. Trace (i) is obtained by scanning the LO phase and trace (iii) by locking to the squeezed amplitude
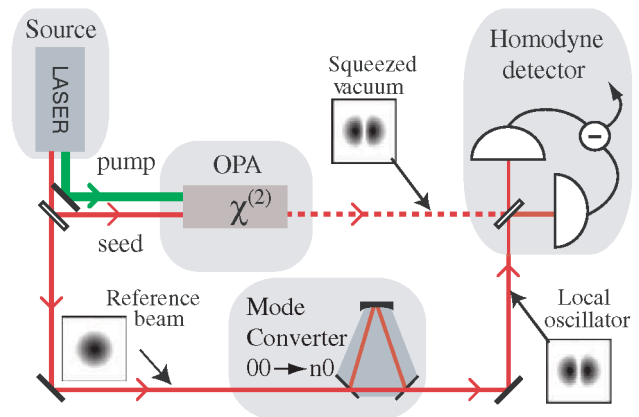

FIG. 3 (color).   Experimental setup to generate TEM$_{n0}$ transverse mode squeezing. An OPA is seeded with an infrared misaligned TEM$_{00}$ beam. The cavity is then locked to the TEM$_{n0}$ mode and pumped with a SH TEM$_{00}$ beam. The TEM$_{n0}$ squeezed beam thereby produced is analyzed using spatial homodyne detection, whose TEM$_{n0}$ LO is created from a misaligned ring cavity. Transverse beam profiles are represented in the case of TEM$_{10}$ mode squeezing.
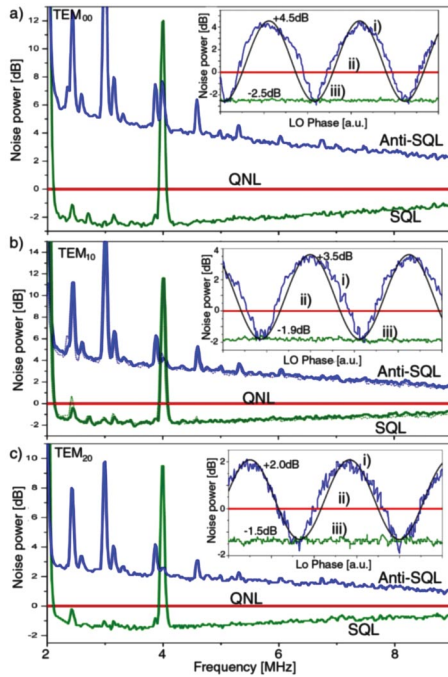
FIG. 4 (color).   Squeezing and antisqueezing spectra measured
in the (a) TEM_{00}, (b) TEM_{10}, (c) TEM_{20} modes. All traces are
taken with a resolution bandwidth of 30 kHz and a video
bandwidth of 30, over more than 1 min. For (b), we also present
the results obtained with a coherent copropagating TEM_{00} mode.
The insets show the noise properties at 4.45 MHz, normalized to
the QNL (ii), when the LO phase is (i) scanned, or (iii) locked to
the squeezing quadrature.

quadrature. We measured squeezing and antisqueezing
values of -2.5 ± 0.4 dB$/ + 4.5 \pm 0.5$ dB for the
TEM_{00}, -1.9 ± 0.3 dB$/ + 3.5 \pm 0.4$ dB for the TEM_{10},
and -1.5 ± 0.3 dB$/ + 2.0 \pm 0.4$ dB for the TEM_{20} mode.
From Fig. 4 can be seen that our squeezed states are almost
pure states, which indicates that the losses are much
smaller then the squeezed states presented in Ref. [30].

We have checked that the detector shows squeezing only
when both LO and resonant mode inside the OPA are set to
the same mode. To prove the feasibility of efficient combi-
nation of such nonclassical fields, we have investigated for
any parasite crosstalk between two orthogonal modes. As
an example, we have compared the nonclassical properties
of a multimode beam, namely, a TEM_{10} squeezed mode,
with and without the presence of a coherent TEM_{00} co-
propagating beam. The great similarity of the spectra
shown in Fig. 4(b) clearly demonstrates that the TEM_{00}
beam does not modify the squeezing and antisqueezing of
the TEM_{10} mode, which is a formal proof that no parasite
crosstalk exists between orthogonal modes.

In summary, our experiments have demonstrated the key
components for multimode parallel quantum information
systems with H-G modes. The encoding of quantum infor-
mation is direct, efficient, and independent since the higher
order modes are exactly linked to the position, momentum,
size, and focussing of a TEM_{00} mode. The quality of

detection of the squeezing in each spatial mode shows
that it is now practical to synthesize a multimode beam
by using our established techniques for lossless mode
combination and analysis (Fig. 1). These results open the
way for quantum information processing with continuous
variables in the transverse plane. The technology for mul-
tiple squeezers driven by one laser is available [32], and we
can now consider the synthesis of multimode beams with at
least five orthogonal modes, each with a pair of quantum
variables (Fig. 1). We are on the way to generate spatially
entangled beams [33] and test the original EPR proposal.
We envision information protocols that are based on par-
allel mode processing and the future challenge is to design
such protocols.

*Electronic address: C.Harb@adfa.edu.au
[1] P. Zoller *et al.*, Eur. Phys. J. D **36**, 203 (2005).
[2] Z. Y. Ou *et al.*, Phys. Rev. Lett. **68**, 3663 (1992).
[3] Ch. Silberhorn *et al.*, Phys. Rev. Lett. **86**, 4267 (2001).
[4] C. Schori *et al.*, Phys. Rev. A **66**, 033802 (2002).
[5] W. P. Bowen *et al.*, Phys. Rev. A **69**, 012304 (2004).
[6] K. McKenzie *et al.*, Phys. Rev. Lett. **93**, 161105 (2004).
[7] H. Vahlbruch *et al.*, Phys. Rev. Lett. **95**, 211102 (2005).
[8] A. Furusawa *et al.*, Science **282**, 706 (1998).
[9] J. Jing *et al.*, Phys. Rev. Lett. **90**, 167903 (2003).
[10] A. M. Lance *et al.*, Phys. Rev. Lett. **92**, 177903 (2004).
[11] V. Josse *et al.*, Phys. Rev. Lett. **96**, 163602 (2006).
[12] S. L. Braunstein *et al.*, Rev. Mod. Phys. **77**, 513 (2005).
[13] H.-A. Bachor and T. C. Ralph, *A Guide to Experiments in
    Quantum Optics* (Wiley, Berlin, 2004).
[14] L. A. Lugiato *et al.*, J. Opt. B **4**, S176 (2002).
[15] C. Schwob *et al.*, Appl. Phys. B **66**, 685 (1998).
[16] S. Gigan *et al.*, J. Mod. Opt. **53**, 809 (2006).
[17] N. Treps *et al.*, Science **301**, 940 (2003).
[18] V. Delaubert *et al.*, quant-ph/0609188.
[19] M. Kolobov *et al.*, Opt. Lett. **85**, 3789 (2000).
[20] I. V. Sokolov *et al.*, Opt. Commun. **193**, 175 (2001).
[21] C. M. Caves *et al.*, Rev. Mod. Phys. **66**, 481 (1994).
[22] A. Zeilinger *et al.*, Science **289**, 405 (2000).
[23] N. K. Langford *et al.*, Phys. Rev. Lett. **93**, 053601 (2004).
[24] H. Kogelnik, "Coupling and Conversion Coefficients for
    Optical Modes," in Proceedings of the Symposium on
    Quasi-Optics, Brooklyn, New York, 1964.
[25] M. T. L. Hsu *et al.*, J. Opt. B **6**, 495 (2004).
[26] V. Delaubert *et al.*, Opt. Lett. **31**, 1537 (2006).
[27] L. A. Wu *et al.*, Phys. Rev. Lett. **57**, 2520 (1986).
[28] P. K. Lam *et al.*, J. Opt. B **1**, 469 (1999).
[29] S. Suzuki *et al.*, Appl. Phys. Lett. **89**, 061116 (2006).
[30] M. Lassen *et al.*, J. Eur. Opt. Soc. **1**, 3 (2006).
[31] A. Vaziri *et al.*, J. Opt. B **4**, S47 (2002).
[32] N. Takei *et al.*, Phys. Rev. A **72**, 042304 (2005).
[33] M. T. L. Hsu *et al.*, Phys. Rev. A **72**, 013802 (2005).